Supplementary Information

Table of Contents

Supplementary Text

Geostationary fire detection

As highlighted in the Materials and Methods, the availability, frequency, and quality of the compiled GOES hotspot data vary over the study area and period.

Given the sequential launch and commissioning of GOES-16 and GOES-17 and the different coverage areas of each satellite, data availability is not consistent across North America between 2017-2020 (Fig. S7A and S7B). The FDCF of Northwestern North America (an area including Alaska and the Yukon) is not imaged by GOES-16, and so hotspot data is only available for this region following the launch of GOES-17 and subsequent FDC product generation (Aug. 2018 to Dec. 2020). Similarly, Northeastern North America is only imaged by GOES-16, so while data are available here for the entire 2017-2020 period, all hotspots identified in this region were solely detected by GOES-16. In central North America, approximately twice as many images and therefore fire products, were available after the launch of GOES-17 and subsequent FDC product generation than beforehand, when the only source of GOES-R hotspots for the region was GOES-16.

During the 2017-2020 period, the scanning mode of GOES-16 and GOES-17 has changed over time to meet changing operational and experimental needs (Fig. S7C and S7D). Availability of full disk imagery, and the FDCF products derived from it, has therefore varied in frequency between 5 minutes (Mode 4), 15 minutes (Mode 3), and 10 minutes (Mode 6). In 2017 and 2018, Mode 3 was the most common operating mode (i.e., 15-minute temporal resolution data), while in 2019 and 2020 Mode 6 was the dominant operating mode (i.e., 10-minute data). As a result, more hotspot data are available for the later part of the 2017-2020 period. For more information on GOES scanning mode specifics see https://www.goes-r.gov/.

As the GOES-R satellites are in geostationary orbits, each ground point location within the study area has a fixed view zenith angle (VZA) with respect to each GOES instrument. VZA

influences the accuracy of fire detection algorithms in several ways[1,2]. For our study, the fact that the hotspot omission error rate increases with VZA required careful consideration and prevented us from performing detailed direct OBE intercomparisons between biomes with very different VZAs.

Overnight burning case studies: 2020 Creek Fire and the 2019 McMillan Complex Fire

As highlighted in Main text and Materials and Methods, we conducted a qualitative analysis of two extreme fire case studies to explore the relationship between the occurrence of OBEs and fire weather dynamics across different biomes: the 2020 Creek Fire (California, Subtropical mountain system) and the 2019 McMillan Complex Fire (Alberta, Boreal).

The Creek Fire burned 154,363 ha, with 43 OBEs observed over 51 days from September 6 to October 27 (Fig. S5). Despite rainfall (3.6mm in total) temporarily halting OBEs on September 18, they quickly resumed the following day due to persistent dryness of moderately slow-drying fuels (DMC) and fuel availability (BUI), highlighting the critical role of drought in facilitating overnight burning. However, non-OBEs can still occur under high DMC and BUI conditions, as seen on October 9 and 10. Many of these non-OBEs are associated with periods of corresponding changes in the fast-reacting variables adverse to fire spread, such as relatively low temperature and increased RH. This also suggested the importance of these variables in OBEs as we found in Fig. S2.

The McMillan Complex Fire burned 199,888 ha, with 9 OBEs within 13 days from May 19 to May 31. Specifically, two OBEs clusters occurred during the McMillan Complex Fire (Fig. S6), centered on May 20 and May 29. During both these periods, DMC and BUI remained relatively low, despite steadily increasing. However, high windspeeds and dry surface fuel at nighttime increased fire spread potential and fire intensity potential, driving OBEs. Although the limited number of spring OBEs in the Boreal prevented further analysis, this qualitative analysis, combined with previous research on spring fires in Alberta[3], suggests that spring

OBEs in the Boreal are likely wind-driven as fuel dryness and availability usually cannot accumulate sufficiently at this time.

Supplementary Figures

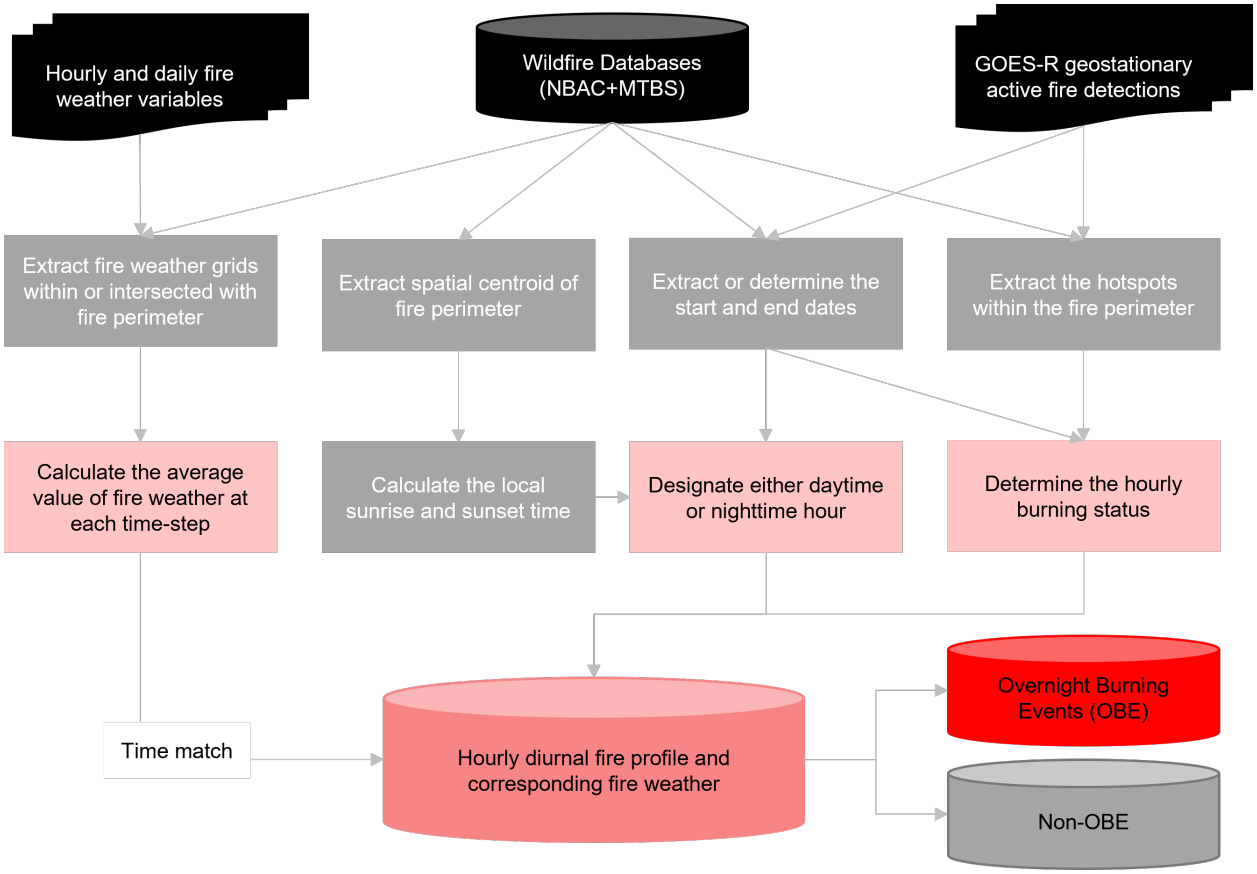

Fig. S1. Data processing workflow used for identifying OBEs and extracting coincident fire weather data.

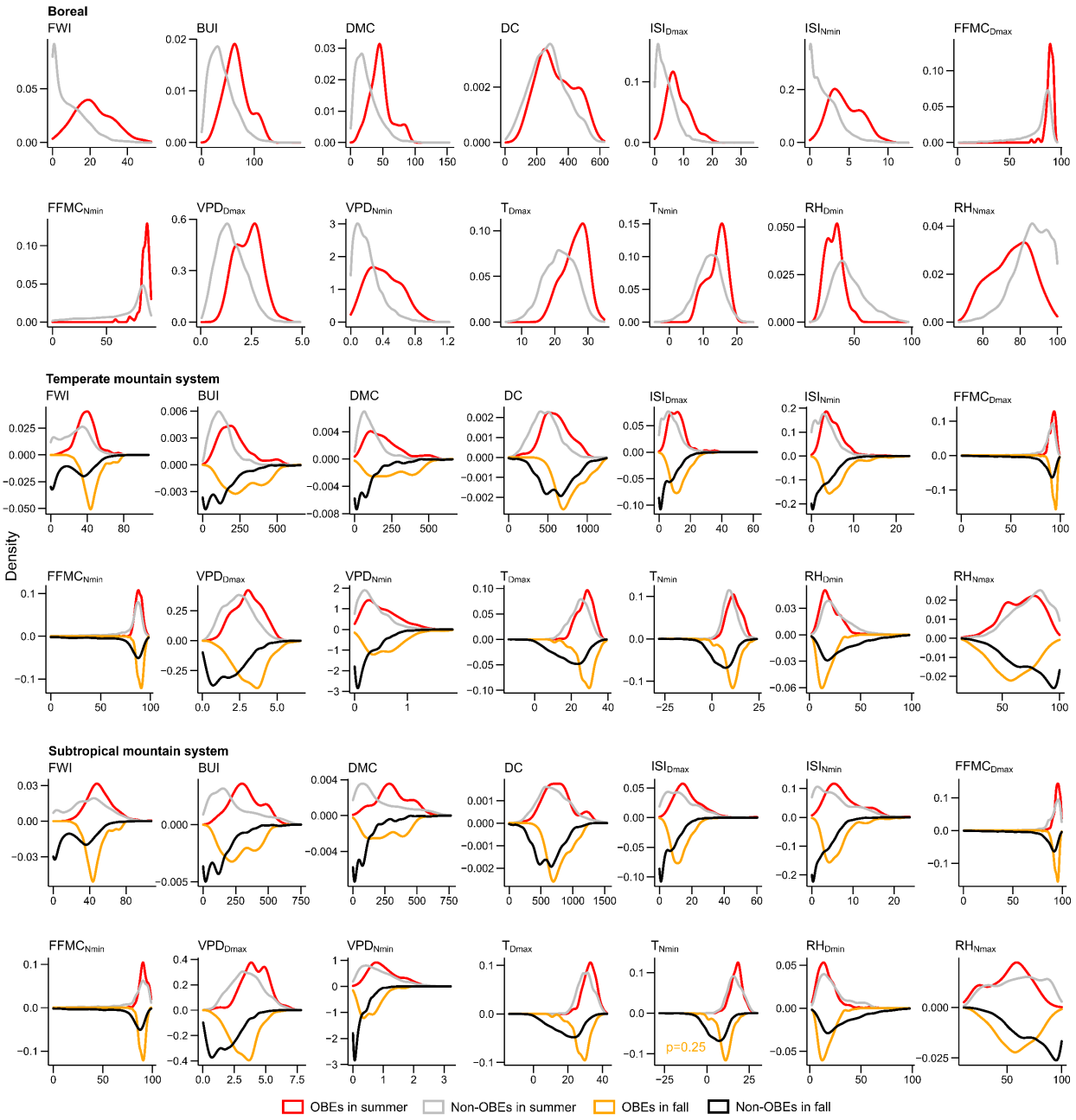

Fig. S2. The supplementary plot to Fig. 3A and 3B. Comparison of fire weather conditions during OBEs and non-OBEs in the Boreal, Temperate mountain system, and Subtropical mountain system. For each biome, curves show the density distribution of daily variables, and daytime and nighttime extremes of hourly variables for OBEs (red for summer and orange for fall) and non-OBEs (gray for summer and black for fall). We invert the y-axis of the distribution of fire weather variables in fall for better visualization. All variables for OBEs in each biome-season group were significantly greater (or smaller in the case of RH; one-sided Mann–Whitney U test, $P < 0.05$) than those for non-OBEs, except T_{Nmin} in Subtropical mountain system fall ($P = 0.25$).

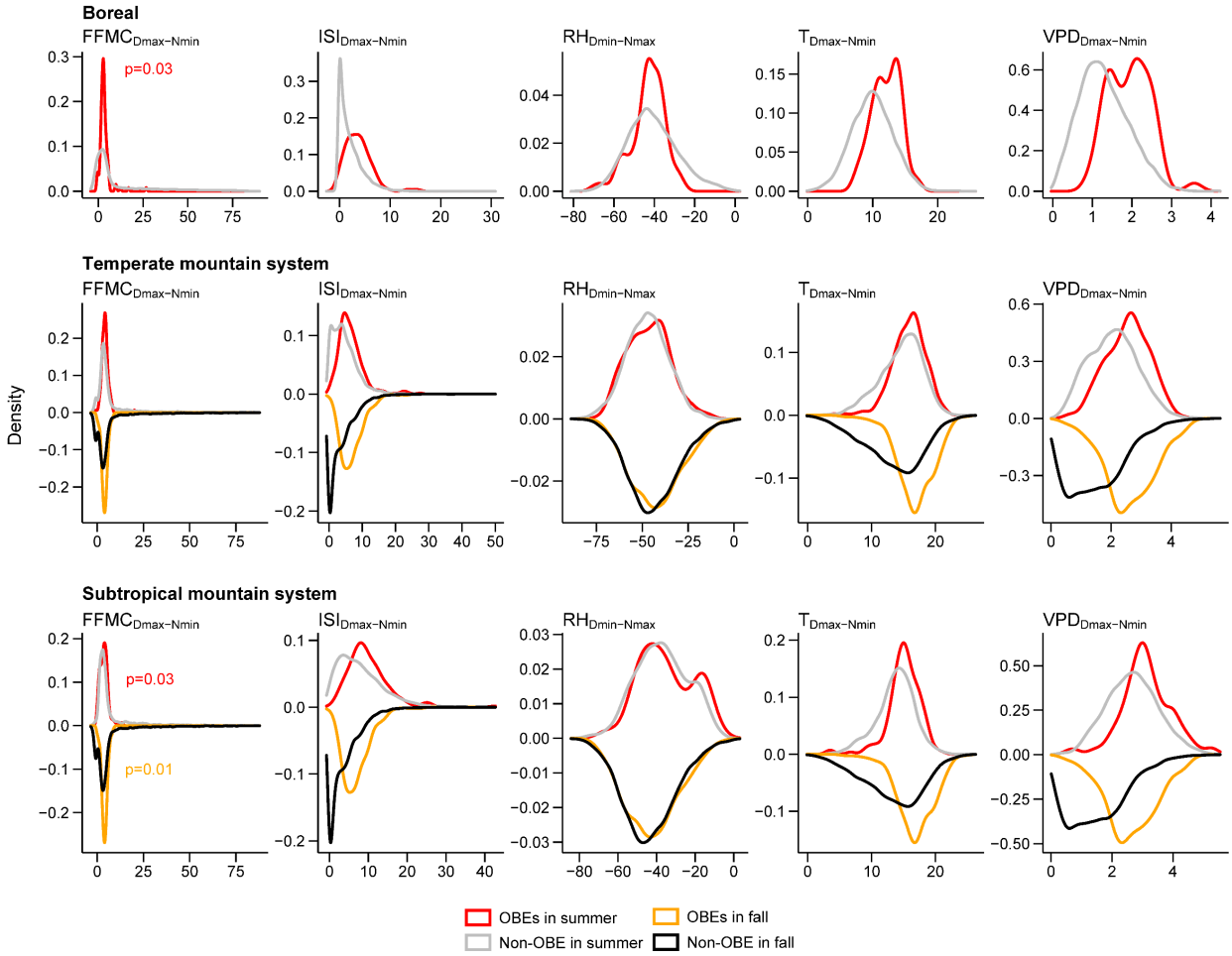

Fig. S3. Comparison of day-night range of hourly fire weather variables (FFMC, ISI, RH, T, and VPD) between OBEs and non-OBEs in Boreal, Temperate mountain system, and Subtropical mountain system. For each biome, curves show the density distribution of day-night ranges for OBEs (red for summer and orange for fall) and non-OBEs (gray for summer and black for fall). We invert the y-axis of the distribution of fire weather variables in fall for better visualization. Only FFMC of OBEs showed a significantly smaller range than non-OBEs (one-sided Mann–Whitney U test, $P < 0.05$) in Boreal summer ($P = 0.03$) and Subtropical mountain system summer (0.03) and fall (0.01).

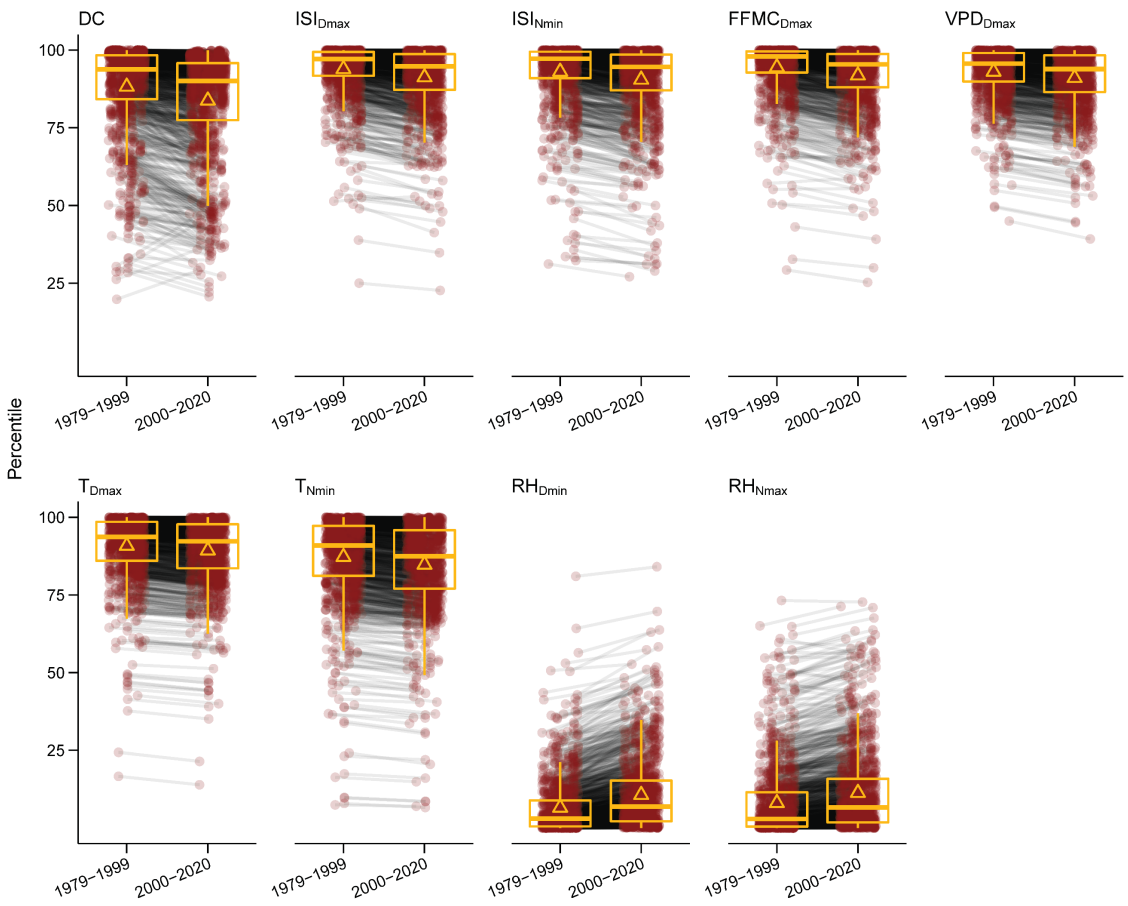

Fig. S4. The supplementary plot to Fig. 3C. The line-linked paired points respectively represent the percentile of fire weather (DC and daytime and/or nighttime extremes of ISI, FFMC, VPD, T, and RH) for each OBE relative to comparable observations during the 1979-1999 and 2000-2020 periods at the same geographic location. The 1979-1999 percentiles are significantly higher than the 2000-2020 percentiles for each fire weather variable (paired Wilcoxon test, $P < 0.05$). Box plots represent the distribution of these percentile values. Each box plot includes a horizontal line to represent the median, a triangle to represent the mean, a box with lower and upper ends that represent the first and third quartiles, and whiskers extending from the corresponding ends of the box to the smallest value at most 1.5 times inter-quartile range and largest value no further than 1.5 times inter-quartile range.

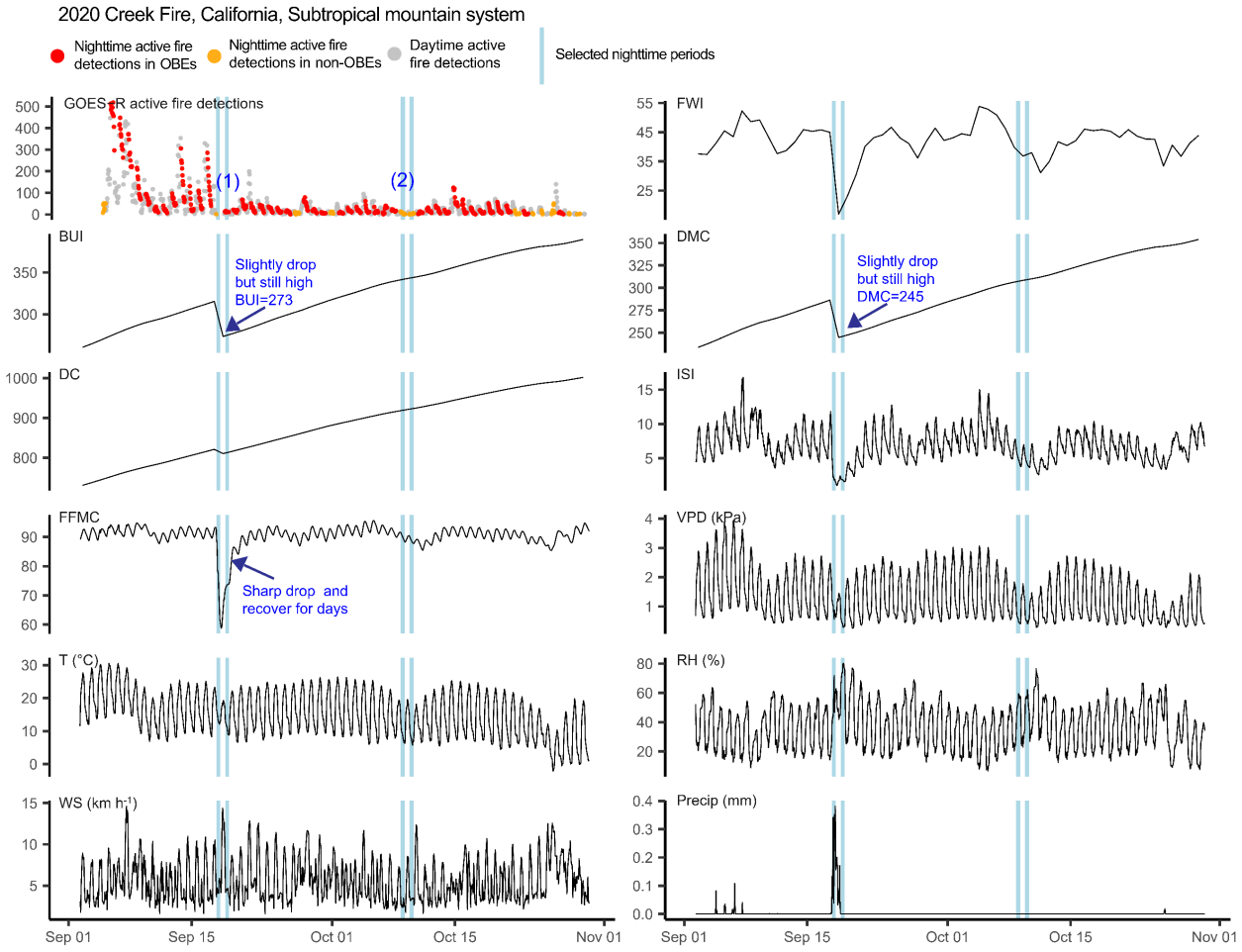

Fig. S5. Active fire detections and coincident fire weather for the 2020 Creek Fire in California, in the Subtropical mountain system biome. The top left shows the time series of GOES-R active fire detection hotspots. Hotspots are categorized and colored according to daytime (gray) and nighttime (red and orange for nighttime hotspots in OBEs and non-OBEs, respectively). The remaining plots show the corresponding fire weather variables as time series. Despite rainfall temporarily putting a stop to OBEs and decreasing fire weather codes and indices on September 18 (see (1)), OBEs quickly resumed on September 19 due to the dryness of moderately slow-drying fuels (DMC) and high fuel availability (BUI). However, non-OBEs can still occur when DMC and BUI were high and unaffected (see (2)). These non-OBEs are associated with periods of corresponding changes in the fast-reacting variables adverse to fire spread, such as relatively low temperature and increased RH.

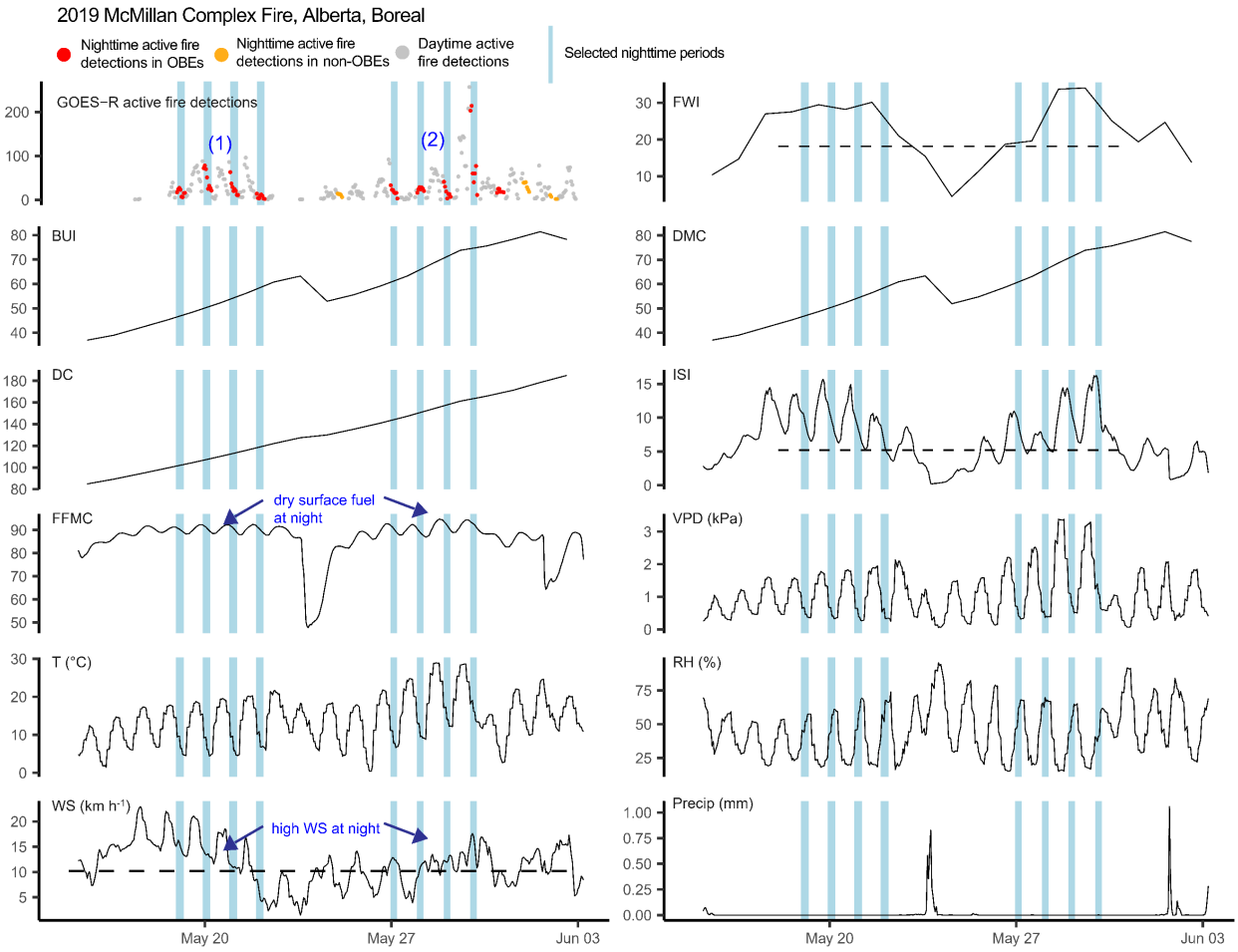

Fig. S6. Active fire detections and coincident fire weather for the 2019 McMillan Complex Fire in Alberta, in the Boreal biome. The top left shows the time series of GOES-R active fire detection hotspots. Hotspots are categorized and colored according to daytime (gray) and nighttime (red and orange for nighttime hotspots in OBEs and non-OBEs, respectively). The remaining plots show the corresponding fire weather variables as time series. Two OBEs clusters occurred during the McMillan Complex Fire centered on May 20 (see (1)) and May 29 (see (2)). During both these periods, DMC and BUI remained relatively low, despite steadily increasing. However, high windspeeds and dry surface fuel (FFMC) at nighttime increased fire spread potential (ISI) and fire intensity potential (FWI), driving OBEs despite low overall fuel availability.

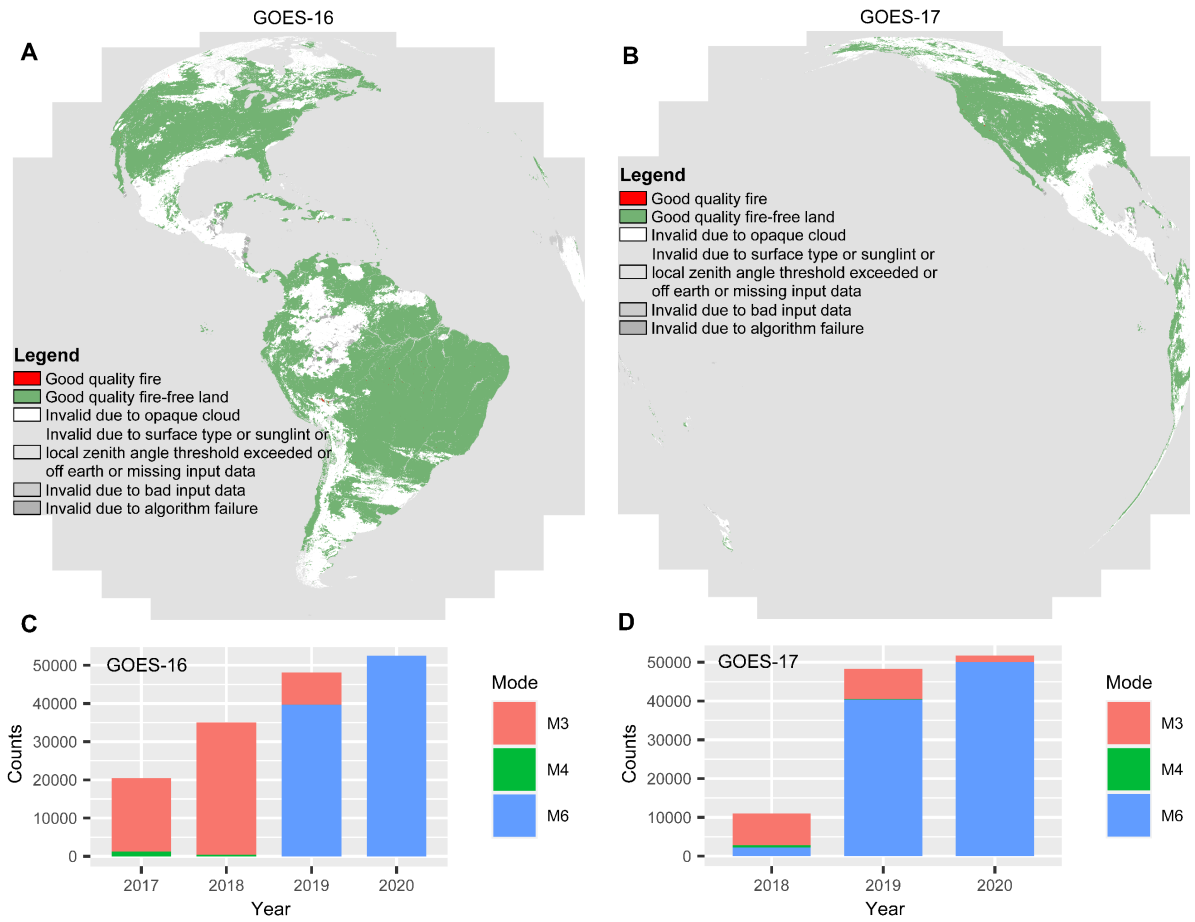

Fig. S7. Coverage and data availability of the GOES-R series Fire/Hot Spot Characterization Full Disk (FDCF) products. Data quality flag layers for (A) GOES-16 (image: 20202500200192000000) and (B) GOES-17 (image: 20202500200319000000) illustrate the spatial extent for the FDCF of each satellite. GOES-16 does not capture the northwestern area of North America and GOES-17 does not capture the northeastern area of North America. (C) and (D) show the number of FDCF products analyzed in this study for GOES-16 and GOES-17, respectively, classified by scanning mode.

Supplementary Tables

Table S1. A summary of the total number of fires with OBEs, all fires, and OBEs by biome. The "single" and "multiple" columns respectively present the number of OBEs from single-OBE fires and multi-OBE fires. The "persistence" column presents the mean number of OBEs for multi-OBE fires. No OBEs were observed in the Temperate oceanic forest biome. Season classifications are as follows: Spring (March-May); Summer (June-August); Fall (September-November); Winter (December-February).

Biome	**Fire with OBEs**	**All fire**	**Total OBEs**	**OBEs by seasons**				**OBEs by fire classes**		**Persistence**
				Spring	Summer	Fall	Winter	Single	Multiple	
Boreal	63	414	145	36	101	8	0	33	112	3.7
Temperate mountain system	126	358	488	1	271	216	0	44	444	5.4
Subtropical mountain system	74	212	330	8	156	165	1	27	303	6.4
Temperate desert	47	247	77	0	64	13	0	34	43	3.3
Temperate continental forest	2	20	4	0	4	0	0	1	3	3
Temperate steppe	6	96	9	3	5	1	0	4	5	2.5
Subtropical desert	6	53	22	3	18	1	0	3	19	6.3
Subtropical dry forest	0	6	0	0	0	0	0	0	0	0
Subtropical humid forest	0	129	0	0	0	0	0	0	0	0
Subtropical steppe	4	100	6	4	2	0	0	3	3	3
Tropical moist forest	2	20	3	3	0	0	0	1	2	2
North America	**330**	**1655**	**1084**	**58**	**621**	**404**	**1**	**150**	**934**	**5.2**

Table S2. The AUC and recall (OBEs) metrics for logistic regression prediction models, organized by variable combination and biome-season group. The highest AUC and recall values are emphasized in bold font. The best models, determined by both AUC (most important criterion) and recall (secondary criterion), are highlighted with a red background.

Combination of variables	**Boreal**		**Temperate mountain system**				**Subtropical mountain system**			
	Summer		Summer		Fall		Summer		Fall	
	AUC	Recall	AUC	Recall	AUC	Recall	AUC	Recall	AUC	Recall
BUI	0.81	73.5%	0.75	63.3%	0.84	72.9%	0.71	63.6%	0.71	**78.6%**
DMC	0.82	75.3%	0.75	59.1%	0.84	69.3%	**0.72**	66.4%	0.72	79.0%
DC	0.61	49.9%	0.72	63.0%	0.74	63.0%	0.57	51.6%	0.60	53.7%
FWI	0.84	73.1%	0.73	71.5%	0.85	**85.7%**	0.67	64.9%	0.73	74.6%
FWI+BUI	0.84	76.4%	**0.77**	70.0%	**0.87**	82.6%	0.70	70.9%	0.72	77.7%
FWI+DMC	**0.84**	76.6%	0.77	69.5%	0.87	81.9%	0.71	71.9%	**0.73**	77.9%
FWI+DC	0.83	73.0%	0.76	**73.2%**	0.85	83.9%	0.67	66.8%	0.73	74.8%
DMC+DC	0.83	**76.7%**	0.75	63.1%	0.84	69.4%	0.71	**72.9%**		
BUI+DC					0.84	72.3%	0.71	72.6%		
FWI+BUI+DC							0.70	72.2%		
FWI+DMC+DC							0.71	72.0%		

Reference in the Supplementary Information

1 Hall, J. V., Zhang, R., Schroeder, W., Huang, C. & Giglio, L. Validation of GOES-16 ABI and MSG SEVIRI active fire products. *Int J Appl Earth Obs* **83**, 101928 (2019).

2 Wooster, M. *et al.* Meteosat SEVIRI Fire Radiative Power (FRP) products from the Land Surface Analysis Satellite Applications Facility (LSA SAF)--Part 1: Algorithms, product contents and analysis. *Atmospheric Chemistry & Physics Discussions* **15** (2015).

3 Tymstra, C., Jain, P. & Flannigan, M. D. Characterisation of initial fire weather conditions for large spring wildfires in Alberta, Canada. *International Journal of Wildland Fire* **30**, 823-835 (2021).